第31卷第1期
2012年2月

红外与毫米波学报
J. Infrared Millim. Waves

Vol. 31, No. 1
February, 2012

文章编号:1001-9014(2012)01-0005-06

Effect of CH_4 flow rate on the optical properties of Boron-doped a-SiC:H films

DOU Ya-Nan[1,2], HE Yue[2], MA Xiao-Guang[2], QIAO Qi[2,3],
CHEN Xiao-Jing[2], WANG Yong-Qian[2], CHEN Robin[2], CHU Jun- Hao[1]

(1. National Laboratory for Infrared Physics, Shanghai Institute of Technical Physics, ChineseAcademy of Sciences, Shanghai 200083, China;
2. Suntech Power Co., Ltd., Shanghai 201114, China;
3. School of Internet of Things Engineering, Jiangnan University, Wuxi 214122, China)

Abstract: The effect of CH_4 flow rate on the structural and optical properties of boron-doped amorphous silicon carbon films as window p-layer in the industrial hydrogenated amorphous silicon solar module was investigated. The p-layer amorphous hydrogenated silicon carbon films were deposited from SiH_4-CH_4 gas mixtures in the Applied Materials SUNFAB radio frequency-plasma enhanced chemical vapor deposition Gen8.5 system with dimensions of 2.2 m 2.6 m. Infrared and transmittance/reflectance spectra were employed to analyze the bond configurations and optical properties of the films associating with structures of the p-layer films which are sensitive to the deposition condition. The optical band gap of the p-layer films increased as the CH_4 flow rate ranged from 3000 sccm to 8850 sccm with other deposition conditions unchanged. With increasing CH_4 flow rate, the deposition rate of p-layer amorphous silicon carbon films decreased slowly, because of the reduction of SiH_3 radical in the SiH_4-CH_4 plasmas. The uniformity of the hydrogenated amorphous silicon carbon films was also investigated, by sampling and analyzing the deposition rate on four different locations of the large area films.

Key words: a-SiC:H; infrared spectrum; uniformity; CH_4 flow rate
PACS: 88.40.jj, 81.05.Gc

甲烷流量对8.5代非晶硅光伏组件P层材料结构和光学性质的影响

窦亚楠[1,2], 何 悦[2], 马晓光[2], 乔 琦[2,3], 陈肖静[2], 王永谦[2], 陈绍斌[2], 褚君浩[1]

(1. 中国科学院上海技术物理研究所 红外物理国家重点实验室, 上海 200083;
2. 尚德太阳能电力有限公司, 上海 201114; 3. 江南大学, 物联网工程学院, 江苏 无锡 214122)

摘要: 本文研究了甲烷流量对作为工业非晶硅光伏组件的p层材料—非晶碳化硅结构和光学性质的影响. p层非晶碳化硅薄膜采用硅烷和甲烷混合气体在射频等离子体增强化学气相沉积(RF-PECVD)设备中沉积制得, 该设备是应用材料公司制造的尺寸为2.2 m × 2.6 m的8.5代系统. 采用红外光谱和透射/反射谱分析与沉积工艺相关的键结构和光学性质. 相同工艺条件下, 当甲烷含量从3000 sccm增加到8850 sccm, p层非晶碳化硅薄膜的光学带隙逐步增加. p层非晶碳化硅薄膜的沉积速率随甲烷流量的增加而逐渐减小, 其原因是硅烷-甲烷等离子体中SiH_3粒子的减少. 文中还通过在不同位置取样和分析沉积速率研究了大面积薄膜的均匀性.

关 键 词: 非晶碳化硅; 红外光谱; 均匀性; 甲烷流量
中图分类号: O484.4 **文献标识码**: A

Introduction

Hydrogenated amorphous silicon (a-Si:H) solar modules have received considerable attention in the in-

Received date: 2011-05-03, **revised date**: 2011-12-23 **收稿日期**: 2010-05-03, **修回日期**: 2011-12-23
Foundation item: Supported by National Natural Science Foundation of China (60821902; U1037604); Foundation of Shanghai talent Program (10PJ1431800)
Biography: DOU Ya-Nan (1983-), male, Weichang, China, Doctor candidate. Research area is silicon solar cells. E-mail: yndou@mail.sitp.ac.cn.

dustrial production market because of their large area and low cost compared with wafer-based silicon solar cells and modules. However, the efficiency of a-Si:H solar cells and modules is very low due to the fabrication processes and light-induced degradation. The monolithic integration of larger-area photovoltaic modules is an efficient way to reduce cost in industrial production. Suntech Power Co., Ltd. introduced a product line based on the Applied Materials SUNFAB technology of RF-PECVD and PVD Gen8.5 system with dimensions of 2.2 m×2.6 m[1].

Amorphous hydrogenated silicon carbon (a-SiC:H) as the window p-layer in a-Si:H solar cells, has been paid much attention because of its wide band gap since 1981 by Tawada et al.[2]. The short circuit current is increased considerably, as films with a wide optical band gap introduces more incident photons into i-layer than that of a-Si:H, and the barrier formed at the p(a-SiC:H)/i(a-Si:H) interface blocks the electrons in the p-layer inversely. The p(a-SiC:H)/i(a-Si:H) heterojunction also increases the open circuit voltage V_{oc} of a-Si:H solar cells because of higher built-in voltage as a result of the wide band gap of a-SiC:H. The structural and optical properties of a-SiC:H films are so severely dependent on the fabrication method and process conditions that some public results are contrary with each other[3-6]. The origin of the increase in the optical band gap related to the microstructure of a-SiC:H films also requires more investigation[6,7,8]. In the mass-production-line, a-SiC:H is the most used window p-layer film material. The aim of the current paper is to study the effect of CH_4 flow rate on the structural and optical properties, such as bond configuration and hydrogen content, optical constants and optical band gap of the p-layer a-SiC:H films deposited in the SUNFAB Gen8.5 RF-PECVD. The uniformity of the a-SiC:H films is also investigated by sampling and analyzing the deposition-rate on four different locations of the 2.2 m×2.6 m thin films.

1 Experimental

Using the gas mixtures of SiH_4, $B(CH_3)_3$, H_2 and CH_4, p-layer a-SiC:H films were deposited by plasma enhanced chemical vapor deposition (PECVD) operating at 13.56 MHz on crystalline Si wafer for infrared, as well as on the large area dummy glass substrate for optical characterization, such as reflectance/transmittance spectra. The SiH_4, $B(CH_3)_3$ and diluted H_2 flow rates denoted by $F(SiH_4)$, $F(B(CH_3)_3)$ and $F(H_2)$ were 8850, 9000 and 42000 sccm, respectively, for all the samples. The total gas pressure in the PECVD chamber was controlled at 2.0 torr. The a-SiC:H films were deposited with the CH_4 flow rate $F(CH_4)$ from 3000 to 8850 sccm under the radiofrequency power density of 50 mW/cm^2 and substrate temperature of 200℃. Sometimes the relative CH_4 concentration in the gas mixtures defined by $R(CH_4) = F(CH_4)/F(CH_4) + F(SiH_4)$ was applied instead of the CH_4 flow rate. Four-group samples including the crystalline Si wafer and dummy glass substrate were obtained to identify the uniformity of large area films, with the sampling locations lying on the sites away from the four corners 600 mm along the long side (2.6 m) and 550 mm along the wide side (2.2 m).

The properties of the a-SiC:H films were studied by infrared absorption, reflectance /transmittance. IR transmission spectra were measured by a commercial Fourier transform infrared spectrometer IFS 66 v/s with KBr beamsplitter at room temperature. The IR absorption spectra related to the structural properties were obtained from the transmission spectra applying the BCC method with baseline correction. FilmTec 3000, with characterization software based on the kinds of material models was used to measure and analyze the transmittance/reflectance to obtain the thickness, optical band gap and optical constants of films.

2 Results and Discussion

A. Variation in the deposition rate

The incident photons absorbed by the p-layer are sensitive to the thickness of the a-SiC:H. The reason is that thicker p-layer absorbing more photons results in more loss of available photons, leading to a smaller current. However, the open circuit voltage V_{oc} increases with the increase in p-layer thickness and becomes saturated until the thickness reaches about 20 nm. Uniformity of thin films is very important for large-area solar modules because of the current match for each

cell in a series and the voltage match between each series-cell isolated by the hot-spot lines. We took four samples near the four corners of each sample, as illustrated in section II. The deposition-rate was calculated from the thickness of a-SiC:H films as a function of relative CH_4 concentration R(CH_4) as shown in Fig. 1. Symbols A to D denote the four sites near the corners of the large-area glass and the corresponding sites in the PECVD chamber. The gas pump is located beside the A/B side several inches away from center, with the line of A to B parallel to the 2.2m direction. Clearly, the deposition-rate at site A/B is higher than that at C/D, and the deposition-rate at each site is a monotonic decreasing function of R(CH_4). Bullot et al. [3] reported that deposition-rate is independent of the gas phase composition before the R(CH_4) reaches 0.8 for the low power density region. For the high power density region, the deposition-rate increases dramatically with the increase in carbon concentration. However, Ambrosone and Coscia [4] and Akaoglu et al. [6] reported the inverse trend for the deposition rate as a function of the relative CH_4 concentration R(CH_4). The result measured in the current paper agrees with that of the latter', except that the deposition rate is at least 2 times higher than that presented in their studies, in which the maximum deposition rate is about 0.3 nm/s. The growth mechanisms of a-SiC:H films are very complex and far from completely understood yet. In the silicon-rich region, the deposition can be explained by the incorporation of SiH_3 radical to the hydrogen terminated on the growing surface under ionic bombardment suggested by Akaoglu et al. [5, 6]. For the gas pump near the A/B site, the mixture update is faster than that at C/D site, so the SiH_3 radical concentration in the plasma is higher thus increasing the deposition rate of films. When the pressure is identical to the total plasma in the chamber, the more the CH_4 concentration in the mixture is, the less SiH_3 radical in the plasma, leading to a smaller deposition rate. Both can be explained by the single radical procedure determined in the growth mode. The dependence of the deposition rate on the relative CH_4 concentration R(CH_4) was also investigated. The linear fitting of deposition-rate versus R(CH_4) is shown in Fig. 1. The slope values are 2.51 for the A/B site and 1.94 for the C/D site. The slope values normalizing to $R = C_{atom}/C_{atom} + Si_{atom}$ in the mixtures calculated from the data given in Ref. 3 and Ref. 6 are presented in the inset of Fig. 1 for comparison. The slope values of 3.46 and 1.89 corresponding to the high-power density of 90 mW/cm^2 and low-power density of 30 mW/cm^2, respectively, in Ref. 6 are similar to the data we obtained at the power density of 50 mW/cm^2. The slopes at the power density of 10 mW/cm^2 and 60 mW/cm^2 are less than 0.5 in Ref. 4 corresponding to a weak dependent.

B. Optical band gap and optical constants

The optical band-gap is very important for the a-SiC:H which is the window layer in p-i-n type solar cells. More photons, with energy between the smaller band gap and the wider band gap, are absorbed by the active i-layer and contribute to the current for the wider band gap a-SiC:H than to the smaller band gap a-SiC:H. Moreover, the p(a-SiC:H)/i(a-Si:H) heterojunction with wider band gap a-SiC:H increases the open circuit voltage V_{oc} of solar cells. However, the incorporation of carbon to increase the optical band gap results in more defects and disorder that degrade the electronic properties of the p-layer, and a heavier lattice mismatching between the p-layer and i-layer or buffer layer. All of these things will lead to severe recombina-

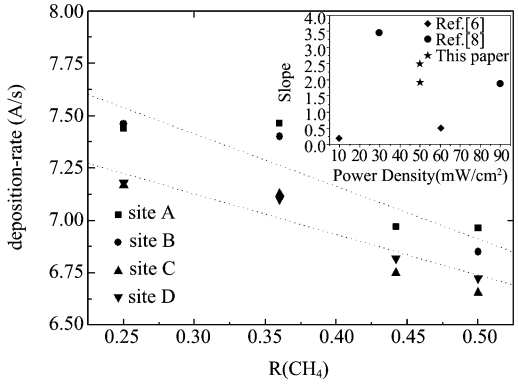

Fig. 1　Deposition rate of the a-SiC:H films as a function of relative concentration R(CH_4). Each series notes the same site in the large-area glass. The dotted lines are the linear fits for the A/B site and C/D site. The inset shows the slopes of the linear fits and slopes calculated from the results in Ref. 4 and Ref. 6

图 1　非晶碳化硅沉积速度随甲烷流量的变化曲线. 每一系列点代表大面积玻璃上的同一位置. 点线是对位置 A/B 和位置 C/D 的线性拟合. 插图是拟合曲线的斜率及文献 6 和 8 中的结果

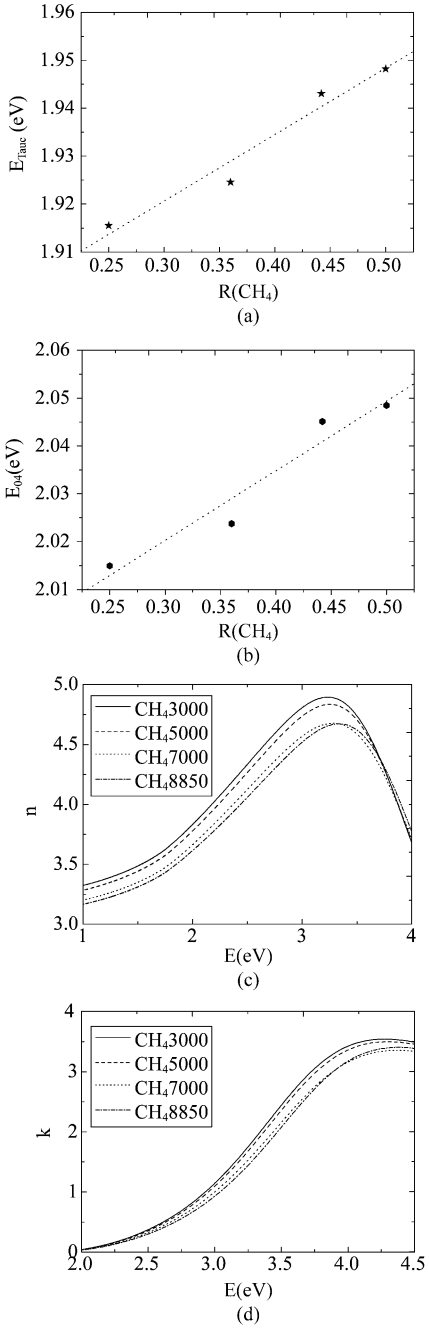

Fig. 2 Optical band gap E_{Tauc} (a) and E_{04} (b) (see text for definition) are plotted as a function of CH_4 relative concentration. Photon energy dependences of optical constants refractive index n and extinction coefficient k are also shown in panel (c) and panel (d)

图2 随相对甲烷流量变化样品的光学带隙 E_{Tauc} (a) and E_{04} (b)(定义由文中给出). 在 c 和 d 中给出折射率 n 和吸收系数 k 随光子能量变化的曲线

tion at the interface. Two methods of determining the optical band gap were applied to show the CH_4 flow rate effect on the optical properties as presented in panel (a) and panel (b) of Fig. 2. Tauc optical band-gap E_{Tauc} is determined by extrapolating a linear part of $(\mathrm{anE})^{1/2} = B_{Tauc}(E - E_{Tauc})$ for $\alpha > 10^3$ cm^{-1} as a function of photon energy E to $\alpha = 0$. Another widely used measure of optical band-gap E_{04} is determined by the energy corresponding absorption coefficient of 10^4 cm^{-1}. From panel (a) and panel (b) of Fig. 2, note that both optical band gaps are proportional to the relative CH_4 concentration in the gas mixtures with a similar factor of 0.14. Spectral dependences of optical constants refractive index n and extinction coefficient k derived from the transmittance/reflectance by the FilmTec 3000 software for different CH_4 flow rate, are also shown in panel (c) and panel (d) of Fig. 2. Over most of the energy band, the n and k decrease as the CH_4 flow rate increases. Note that, the extinction coefficient below the optical band gap is unreliable because the TL model used by the software does not contain the parts of defect absorption and Urbach tail absorption at low energy. Optical properties are related to the structure of a-SiC:H films, such as compositions, microcrystalline, hydrogen content and bond configurations, and void density. In a-Si:H films, the increase in optical band gap is primarily caused by the alloying effect and improving order for hydrogen incorporation[7]. However, Raman spectrum (not presented here) shows that the degree of disorder increased weakly as the CH_4 flow rate increased, which could be duo to the carbon incorporation leading to the enhancement of the bond angle distortion, as Si-C bonds are much shorter than Si-Si bonds[8]. As Akaoglu et al. reported, the effects of the microcrystalline phase and void density on optical properties are insignificant[6]. Thus the widening of the optical band-gap may be resulted from the alloying effect, i. e., the incorporation of hydrogen and carbon, through the replacement of weaker, strained Si-Si bonds by stronger Si-H_n bonds and/or Si-C bonds[7,8], as confirmed by the IR spectra in the next subsection. Decrease in refractive index and extinction coefficient is attributed to the increase in atomic carbon fraction in the films.

The lattice mismatching is not serious in the preparation of the amorphous silicon solar module with a thin buffer layer inserted between the p-layer and i-layer. Thus the CH_4 flow rate of 8850 sccm, with the wi-

dest optical band gap in the flow rates studied may be a good choice for the p-layer a-SiC:H. Considering the deposition rate and material cost, a larger CH_4 flow rate is not necessary.

C. IR spectra analysis

IR spectroscopy, a simple and nondestructive technique, was used to obtain the information of hydrogen content and bonds configuration. Most of the bond vibration modes were identified (for more details, see Ref. 6.). Fig. 3 presents the IR absorption of the a-SiC:H thin films deposited at four different CH_4 flow rates from 3000 sccm to 8850 sccm, with the wavenumber ranging from 600 cm^{-1} to 800 cm^{-1}, 1900 cm^{-1} to 2200 cm^{-1}, and 2800 cm^{-1} to 3000 cm^{-1}. The relative IR absorption in Fig. 3 (a) shows that the vibration mode around 770 cm^{-1}, i. e., Si-C stretching or Si-CH_3 wagging mode enhances obviously as the CH_4 flow rate increases, indicating the enhancement of Si-C bonds density. The stretching modes of C-H_n, which were distributed in the energy range of 2800 cm^{-1} to 3000 cm^{-1}, containing three peaks of 2850, 2920, and 2960 cm^{-1}, are shown in panel (b) of Fig. 3. The increase in the CH_4 flow rate results in an enhancement of these modes densities. Owing to the higher electronegativity of the carbon atom, the peak at 2000 cm^{-1} shifts toward the higher wave number band when the carbon atoms attach to silicon[2, 6], as shown in the Fig. 3 (c). The fitting curves with two Gaussian functions centering at 2000 cm^{-1} and 2060 cm^{-1} to 2100 cm^{-1} for the Si – H_n and $(Si\text{-}H_2)_n$ vibration modes, are presented in Fig. 3(c). The peak at 2000 cm^{-1} is attributed to the Si-H stretching mode[6]. While the peak at 2060 ~ 2100 cm^{-1} range is contributed from Si-H_2 stretching and/or CSi-H stretching[2]. Note that the peak positions of the fitting function at a higher frequency is shifted from 2081 cm^{-1} to 2071 cm^{-1}. No remarkable enhancement occurred in the wave number range of 850 cm^{-1} to 900 cm^{-1} corresponding to the $(Si\text{-}H_2)_n$ bending mode. Thus, the vibration mode at a higher frequency could be enhanced partly by the CSi-H stretching mode whose calculated centering frequency was at 2054 cm^{-1}[2]. That is an enhancement of carbon atom density in the film occurred with the increase in CH_4 flow rate. Si-H_2 bond

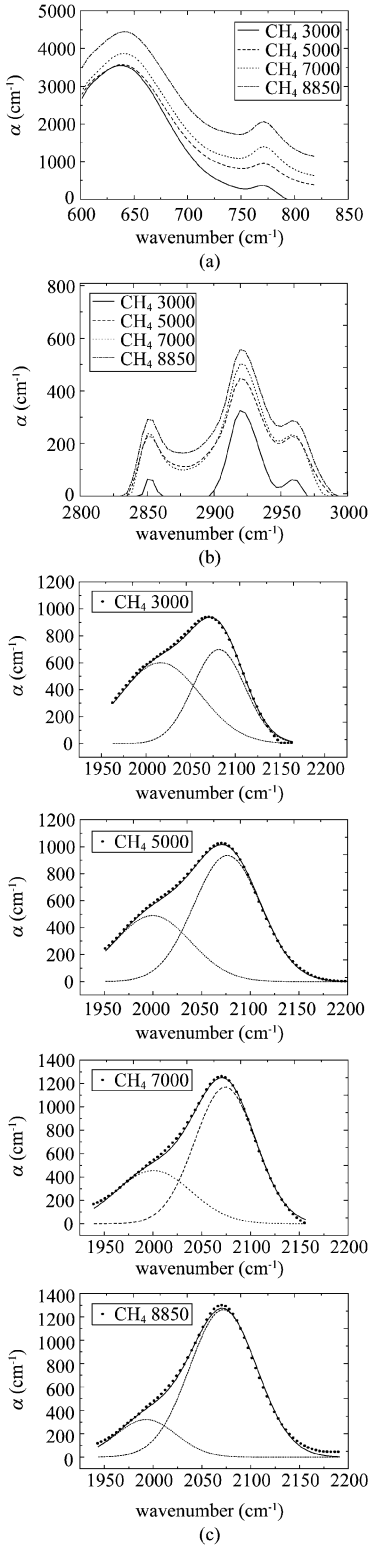

Fig. 3　IR absorption bands of the a-SiC:H films in the wave number ranges of (a) 600 cm^{-1} to 800 cm^{-1} and (b) 2800 cm^{-1} to 3000 cm^{-1} and (c) 1900 cm^{-1} to 2200 cm^{-1}. The fit with two Gaussian-shaped functions for the Si-H_n and $(Si\text{-}H_2)_n$ stretching modes are also shown in (c)

图 3　非晶碳化硅薄膜在 (a) 600 ~ 800 cm^{-1} (b) 2800 ~ 3000 cm^{-1} and (c) 1900 ~ 2200 cm^{-1} 的吸收谱. 用两个高斯函数对振动键 Si-H_n 和 $(Si\text{-}H_2)_n$ 的拟合曲线显示在(c)中

is generally considered a major cause of dangling bonds, which are the origin of light-induced degradation. In the window p-layer of p-i-n solar cells and modules, the thickness is only about 10 nm, thus, light-induced degradation can be negligible. Hydrogen concentration can be calculated from the integrated absorbance through $N_H = A\int(\alpha/\omega)\,d\omega$ in the band range of the wagging or stretching vibration mode, with $A_{s_1} = 9.0\times10^{19}$ cm^{-2} and $A_{s_2} = 2.2\times10^{20}$ cm^{-2}, where the subscripts s_1 and s_2 denote the Si-H stretching mode at 2000 cm^{-1} and the Si-H_2 stretching mode at 2060 cm^{-1} to 2100 cm^{-1}, respectively. For simplicity, the hydrogen content of at. % is normalized to the crystalline Si density of 5.0×10^{22} cm^{-3}; it is plotted in the inset of Fig. 4. The relative CH_4 concentration increase in the gas mixtures resulted in the increase in hydrogen content from 16 at. % to 25 at. %. The results confirm that the origin of the increase in optical band-gap is the incorporation of carbon and hydrogen through the replacement of weak Si-Si bonds by Si-H_n and Si-C bonds. However, the part contributed by Si-H decreases slowly from 6% to 2%, as shown in the inset of Fig. 4. The ratio of hydrogen concentration related to Si-H and Si-H_2/SiC-H is also presented in Fig. 4, which is a monotonic decrease as a function of the relative CH_4 concentration in gas mixtures.

3 Conclusions

The uniformity, deposition-rate, and structural and optical properties of a-SiC:H deposited at a CH_4 flow rate in the range of 3000 sccm to 8850 sccm by Gen8.5 PECVD in SiH_4-CH_4 gas mixtures were investigated. The deposition rate at the site near the pump is slightly higher than that at the site distant away from the pump, leading to a uniformity of about 10 %. The increase in the CH_4 flow rate results in the reduction of the deposition rate because of the decrease in SiH_3 radical ratio in the SiH_4-CH_4 plasma in the single radical procedure frame. The optical band gap, determined by Tauc plot and absorption coefficient, increases with the increase of CH_4 relative concentration because more weak Si-Si bonds are substituted by the stronger Si-H_n and Si-C. Moreover the optical constants, refraction index, and extinction coefficient decrease in most of the photon energy band.

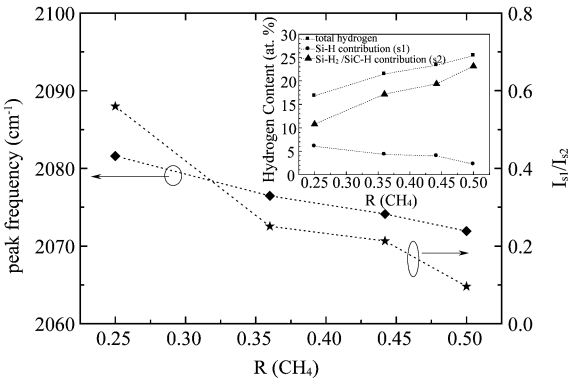

Fig. 4 Peak position of fitting Gaussian function in the energy range of 2050 cm^{-1} to 2010 cm^{-1} and ratio of hydrogen content contributed to Si-H Is_1 and Si-H_2/SiC-H Is_2 are plotted as a function of relative CH_4 concentration. The inset reports the evolution of total hydrogen content as well as the contributions related to the Si-H and Si-H_2/SiC-H

图4 高斯拟合函数的峰值位置和对振动键 Si-H 和 Si-H_2/SiC-H 有贡献的氢含量比值随相对甲烷流量的变化曲线. 插图表示总氢含量及对 Si-H 和 Si-H_2/SiC-H 有贡献的氢含量随相对甲烷流量增加的变化曲线

REFERENCES

[1] Vetter M, Borrajo J P, and Andreu J. Fabrication of very large 2.6 m × 2.2 m amorphous silicon olar modules on glass[C]. *Proceedings of the* 2009 *Spanish Conference on Electron Devices*, 2009, 406 – 409.

[2] Tawada T, Tsuge K, Kondo M *et al.* Properties and structure of a-SiC:H for high-efficiency a-Si solar-cell[J]. *Journal of Applied Physics*, 1982, **53**(7): 5273 – 5281.

[3] Bullot J and Schmidt M P. Physics of amorphous-silicon carbon alloys[J]. *Physica Status Solidi B-Basic Research*, 1987, **143**(2): 345 – 418.

[4] Ambrosone G, Coscia U, Ferrero S *et al.* Structural and optical properties of hydrogenated amorphous silicon-carbon alloys grown by plasma-enhanced chemical vapour deposition at various rf powers[J]. *Philosophical Magazine B-Physics of Condensed Matter Statistical Mechanics Electronic Optical and Magnetic Properties*, 2002, **82**(1): 35 – 46.

[5] Akaoglu B, Gulses A, Atilgan I *et al.* Influences of carbon content and power density on the PECVD grown a-Si_{1-x}:C_x: H thin films[J]. *Vacuum*, 2006, **81**(1): 120 – 125.

[6] Akaoglu B, Sel K, Atilgan I, *et al.* Carbon content influence on the optical constants of hydrogenated amorphous silicon carbon alloys[J]. *Optical Materials*, 2008, **30**(8): 1257 – 1267.

[7] Maley N and Lannin J S. Influence of hydrogen on vibrational and optical-properties of a-$Si_{1-x}H_x$ alloys[J]. *Physical Review B*, 1987, **36**(2): 1146 – 1152.

[8] Mui K, Basa D K, Smith F W. *et al.* Optical-constants of a series of amorphous hydrogenated silicon-carbon alloy-films-dependence of optical-response on film microstructure and evidence for homogeneous chemical ordering[J]. *Physical Review B*, 1987, **35**(15): 8089 – 8102.